Available online at www.sciencedirect.com
ScienceDirect
Journal of the European Ceramic Society 28 (2008) 829–835
www.elsevier.com/locate/jeurceramsoc

Electrical barriers formation at the grain boundaries of Co-doped SnO_2 varistor ceramics

R. Metz [a,b,*], D. Koumeir [a], J. Morel [a], J. Pansiot [a], M. Houabes [a], M. Hassanzadeh [c]

[a] *Laboratoire Hydrazines et Procédés Lyon1-CNRS-Isochem (Groupe SNPE), UMR 5179, université Claude Bernard Lyon 1, Bâtiment Berthollet, 22 Avenue Gaston Berger, 69 622 Villeurbanne, France*

[b] *Institut Charles Gerhardt, UMR 5253 Université Montpellier 2 composante Physicochimie des Matériaux Organisés Fonctionnels, CC 1700, Place Eugène Bataillon, 34095 Montpellier Cedex 5 - FRANCE*

[c] *Areva T&D, DRC 1340 rue de Pinville, 34965 Montpellier Cedex 2, France*

Received 8 March 2007; accepted 17 May 2007
Available online 19 November 2007

Abstract

The nonlinear electrical properties of CoO-doped SnO_2 ceramics were characterized. A second phase is observed at the surface of the microstructure of the specimens. Energy-dispersive X-ray analysis reveals that the second phase is composed of tin, cobalt and oxygen with an approximate atomic ratio estimated for Co and Sn: 2:1. The phase was identified by X-ray diffraction and unambiguously establish the identity of the phase: Co_2SnO_4. Electrical characterization of the binary CoO–SnO_2 was carried out on a very large range of current from 10^{-9} up to 100 A cm^{-2} showing that the doping of CoO increases drastically the resistivity of the ceramic from 10^4 to 10^{10} Ω cm. This value appears to be a threshold for which the nonlinear effect appears.

Keywords: Varistors; SnO_2; Electrical properties; Grain boundaries

1. Introduction

SnO_2 ceramics are n-type semi-conductors with native oxygen vacancies compensated by electrons: $O_0^x = 2e + V_0'' + (1/2)O_2(g)$. Tin oxide ceramics have many uses such as gas sensors, electrodes for electric glass melting furnaces, electrochromic devices, crystal displays, photodetectors, solar cells and protective coating. Recently in 1995, a new application has emerged as varistor[1] (a varistor device is a nonlinear resistor displaying a nonohmic current–voltage behaviour, which can be used as a voltage protector device). More than 100 papers have been since written sensing that this new polycrystalline ceramics SnO_2 as emerging for potential application as commercial devices. However the use of tin oxide ceramics is limited as dense ceramic since it is hard to densify because evaporation and condensation, which promote coarsening and grain growth, mostly dominate mass transport.[2–4]

Several sintering aids have been used to improve the densification of SnO_2 ceramics.[4,5] CoO was reported as one of the effective dopants.[6] To explain the promotion of mass transport in SnO_2, it is suggested that Co^{2+} creates oxygen vacancies in the SnO_2 lattice by substitution to tin: $CoO \rightarrow Co_{Sn}'' + V_0^{\circ\circ} + O_0^x$. This doping gives additional defects in the structure. It is believed that the vacancies are preferentially created at the surface of the SnO_2 grains, increasing oxygen diffusion at grain boundaries and then promoting densification.[7]

Although multi-components system such as SnO_2–CoO–Nb_2O_5–Cr_2O_3 lead apparently to single-phase ceramics,[1] in the binary system CoO–SnO_2 the solid solution limit seems very weak since polyphased ceramics are obtained.[6] The ionic radius mismatch between Co and Sn is very small ($r_{Co^{2+}} = 0.074$ nm, $r_{Sn^{4+}} = 0.071$ nm, $\Delta r = 0.003$ nm). Despite a very weak mismatch, the solid solution limit between SnO_2 and CoO is exceeding even up 0.5%$_{mol}$ leading to the precipitation of

* Corresponding author.
E-mail address: metz@univ-lyon1.fr (R. Metz).

0955-2219/$ – see front matter © 2007 Elsevier Ltd. All rights reserved.
doi:10.1016/j.jeurceramsoc.2007.05.024

Co_2SnO_4.[6] This phase is also reported by electronic diffraction.[6] It is located in the grain boundaries[6] and appears on cooling at the ceramic surface.[8]

The lattice parameters of SnO_2 was measured by Fayat and Castro[9] $a = 0.4738$ nm and $c = 3.185$ nm ($V = a^2c = 0.715\ nm^3$). 0.5%$_{wt}$ CoO addition to SnO_2 system produces an increase in the lattice volume up to 7.157 nm^3.[9]

Tin oxide presents intrinsic and extrinsic defects. As intrinsic defect, the formation of a Schottky pair on two new sites in the crystal surface can be described as

$$Sn_{Sn}^{x} + O_0^{x} \leftrightarrow V_0^{\circ\circ} + V_{Sn}'' + Sn_{Sn}^{x} + O_0^{x}$$

Or more simply:

$$\text{perfect crystal} = V_0^{\circ\circ} + V_{Sn}''$$

The electronic defects in an intrinsic semi-conductor:

$$\text{perfect crystal} = \acute{e} + h^{\circ}$$

Nonstoichiometry of tin oxide ($SnO_{2-\delta}$) appears above 1173 K ($\delta = 0.03$)[10]:

$$O_0^{x} = (1/2)O_2 + V_0^{\circ\circ} + 2\acute{e}$$

The substitution of cobalt II (ionic radius 0.072 nm) to tin IV (ionic radius 0.071 nm) lead to the creation of a positively charged oxygen vacancy according to

$$CoO \rightarrow Co_{Sn}'' + V_0^{\circ\circ} + O_0^{x}$$

Both electrostatic (coulomb forces between individual defects) and elastic interactions can be decreased by an association of the defects. Kim et al.[11] considered that the elastic interactions can be neglected since the size mismatch between Co^{2+} and Sn^{4+} is very weak. This has been confirmed by ab initio calculs which show that the defect associate $[Co_{Sn}'' + V_0^{\circ\circ}]$, due to their columbic attraction, is stabilized in the SnO_2 lattice.[12] Extrinsic oxygen vacancies–cobalt ions associates form shallow donor levels below the conduction band. Precipitation of Co_2SnO_4 phase is explained by an observed diffusion of Co_{Sn}''. The oxidation reaction $(1/2)O_2 + V_0^{\circ\circ} + 2\acute{e} \rightarrow O_0^{x}$ at the surface of the specimens imposes a concentration gradient of oxygen vacancies between the surface and the interior of the CoO-doped SnO_2 sinter body. The concentration of oxygen vacancies at the sample surface is lower due to outward-diffusion of associate defects. At the same time, since both point defects diffuse together, the concentration of cobalt ions at the surface is increased and exceeds the solubility limit of Co ions in SnO_2. Therefore Co_2SnO_4 phase is precipitated on the surface.

The purpose of the present work is to study the effects of CoO on the electrical properties of SnO_2 with the aim to obtain both high-density ceramic and good electrical properties.

2. Experimental procedure

The oxides used in this study were analytical grade SnO_2 (Alfa Aesar 99.9%), CoO (Alfa Aesar 99.7%). The composition $SnO_2 + x\%_{wt}$ CoO (x varying from 0 to 2) was obtained by conventional mixing using a ball mill. The oxide powders were then mixed with a polyvinyl alcohol binder, granulated and pressed into pellet shapes. The powders were isostatically pressed at a pressure of 7×10^9 Pa during 1 s. The samples were then sintered in ambient air atmosphere at 1623 K for 2 h and slowly cooled to ambient temperature. They were heated at a rate of 120 K/h to the sintering and room temperature. Densities were determined by geometrical measurement of the volume and by weighing the pellets using an analytical balance.

The densification of the specimens after sintering at 1623 K during 2 h is calculated starting from the following formula:

$$D = \left(\frac{\rho}{\rho_{th}}\right) \times 100$$

with ρ = apparent density of the pellet (g/cm^3) and ρ_{th} = theoretical density of pure SnO_2.

Silver electrodes are fired at 873 K (800 K/h up to 873 K), the electric characteristics of the components are depicted on Fig. 3.

Microstructural characterization of sintered samples was made by scanning electron microscopy (Hitachi S 800 and XL30 ESEM Philips coupled with energy-dispersive spectroscopy (EDS–EDAX). Ceramic patterns were recorded on a Bruker D8 Advance Diffractometer (Cu $K_{\alpha 1,\alpha 2}$) equipped with a Vantec detector and a spinner.

For the electrical measurements, silver contacts were deposited on the samples surfaces, after which the pellets were heat treated at 873 K for several minutes. To determine the electrical properties as a function of temperature a special sample holder was built and attached to an electrical source and two digital multimeters for current higher than 1 mA cm^{-2}, the current–voltage measurements were taken using a high voltage-measuring unit using a current generator which delivers a 8/20 μs impulse current with a peak short-circuit of 6 kA. The nonlinear coefficient was obtained by linear regression of the experimental points using a logarithmic scale around 1 mA cm^{-2} and the breakdown electrical field was obtained at this current density. The nonlinear coefficient α, for all the samples studied, were estimated between two desired magnitudes of current and corresponding voltage by $\alpha = \log(J_{0.1\ mA/cm^2}/J_{1\ mA/cm^2})/\log(E_{0.1\ mA/cm^2}/E_{1\ mA/cm^2})$, where $E_{0.1\ mA/cm^2}$ and $E_{1\ mA/cm^2}$ are voltage fields at current densities, J, at 0 1 mA/cm^2 and 1 mA/cm^2 respectively.

3. Results and discussion

In order to investigate the role of cobalt monoxide on the electric properties of SnO_2-based varistors, we studied the SnO_2 composition with x% in mass of CoO and x varying from 0 to 2%$_{wt}$ (Table 1).

The results of the densification according to the cobalt monoxide content before and after sintering are depicted in Table 2. Pressed compact of pure tin oxide does not densify. This result indicates that the surface energy is insufficient to cause appreciable sintering. Pressing did not introduce sufficient strain energy to increase the sintering rate. Doping by only 0.25% cobalt monoxide causes the ceramic densification. This indicates that cobalt oxide is extremely effective in promot-

Table 1
Studied formulations: SnO_2–CoO

Composition	SnO_2		CoO	
	wt.%	mol%	wt.%	mol%
1	100	100	0	0
2	99.95	99.9	0.05	0.1
3	99.75	99.5	0.25	0.5
4	99.5	99	0.5	1
5	99	98.01	1	1.99
6	98.5	97.03	1.5	2.97
7	98	96.06	2	3.94

Table 2
Densification with vintage before and after sintering according to the content cobalt oxide (sintering: 1623 K during 2 h at a rate of 120 K/h up and down)

CoO (%)	Densification (%)	
	Before sintering	After sintering
0	66 ± 2	66 ± 2
0.05	63 ± 2	74 ± 2
0.25	66 ± 2	98 ± 2
0.5	64 ± 2	93 ± 2
1	66 ± 2	94 ± 2
1.5	66 ± 2	93 ± 2
2	65 ± 2	89 ± 2

ing densification of SnO_2, even for weak dopants concentrations.

Cerri et al.[13] found that the maximum of linear contraction ($d(\Delta L/L_0)/dT$) depends on the concentration of dopants. Addition of 0.5, 1 and 2%$_{mol}$ of CoO onto SnO_2 show that the intermediate doping of 1%$_{mol}$ gave the greatest linear shrinkage. Our results obtained with other experimental conditions confirm this point: the amount of cobalt oxide in the ceramic has to be accurately tuned in order to promote the best densification. In our experimental conditions, 0.25%$_{wt}$ of cobalt oxide gave 98% of the theoretical density although 2%$_{wt}$ gave a poor value of 89% (Fig. 1). The high densification observed in the CoO-doped SnO_2 can be explained by the substitution of Sn^{4+} ions by Co^{2+}

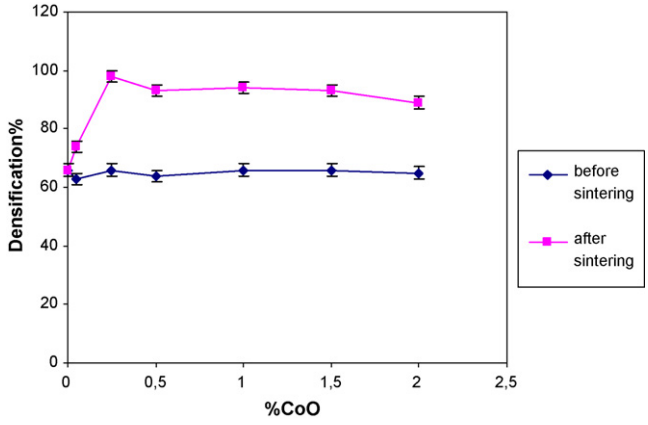

Fig. 1. Apparent densification according to the content cobalt monoxide.

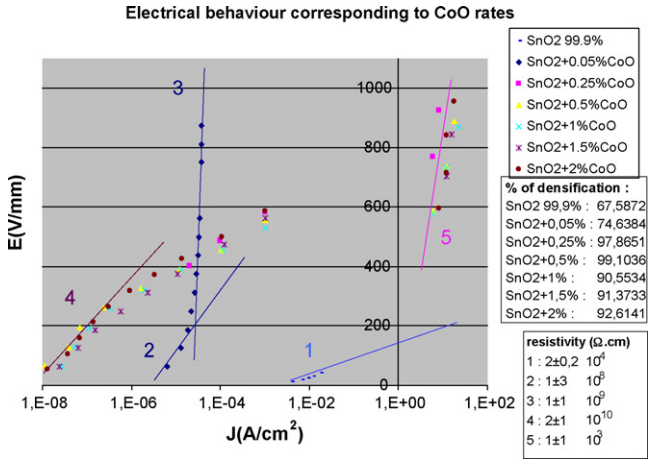

Fig. 2. Electric field according to the current density for different cobalt doping (sintering stage: 1623 K during 2 h).

in the SnO_2 crystalline lattice:

$$CoO \xrightarrow{SnO_2} Co''_{Sn} + V''_0 + (1/2)O_2$$

The formation of oxygen vacancies would help mass transport in SnO_2 lattice.

Fig. 2 shows the electrical field versus current density. Undoped tin dioxide behaves like a resistance. Its coefficient of nonlinearity (α) is close to 0. The presence of cobalt monoxide in the formulation results in the appearance of a zone of nonlinearity with coefficients varying from 11 to 18 (Table 3).

The leakage current decreases from $x = 0$ to 0.25 and tends to be stabilized towards 5×10^{-7} A cm^2 for $x \geq 0.5$. X-ray diffraction (XRD) of the sintered sample shows there is no secondary phase (Fig. 3A), since only the SnO_2 phase was detected.

In order to appreciate the height of the barrier of potential to the grain boundaries, we characterized the samples at temperatures varying from ambient to 448 K. The characteristics are depicted as the curve $\ln J = f(E^{1/2})$ for each temperature and are provided for only the composition 0.5%$_{wt}$ of CoO (Fig. 4). The electrical conductivity increases linearly with increasing temperature. For low values of $E^{1/2}$ the curves are straight lines and the extrapolation of these lines in the ohmic area with $E = 0$ gives the values of the density of current ($\ln J$) for various temperatures. Generally the leakage current is given by the relation:

$$J = AT^2 \exp\left[\frac{\beta E^{1/2} - \Phi}{KT}\right]$$

Table 3
Electrical parameters in function of the cobalt oxide cobalt content (leakage current (J_F)), (field of threshold (E_s)) and (nonlinear coefficient (α))

CoO (%)	J_F (A cm^{-2})	E_s (V/mm)	α
0	4 ± 1E−04	55 ± 30	1 ± 2
0.05	9 ± 3E−06	1161 ± 91	0 ± 2
0.25	2 ± 1E−04	657 ± 75	11 ± 2
0.5	5 ± 1E−07	542 ± 33	14 ± 2
1	5 ± 3E−07	540 ± 34	18 ± 2
1.5	5 ± 1E−07	572 ± 10	13 ± 2
2	3 ± 2E−07	820 ± 90	14 ± 2

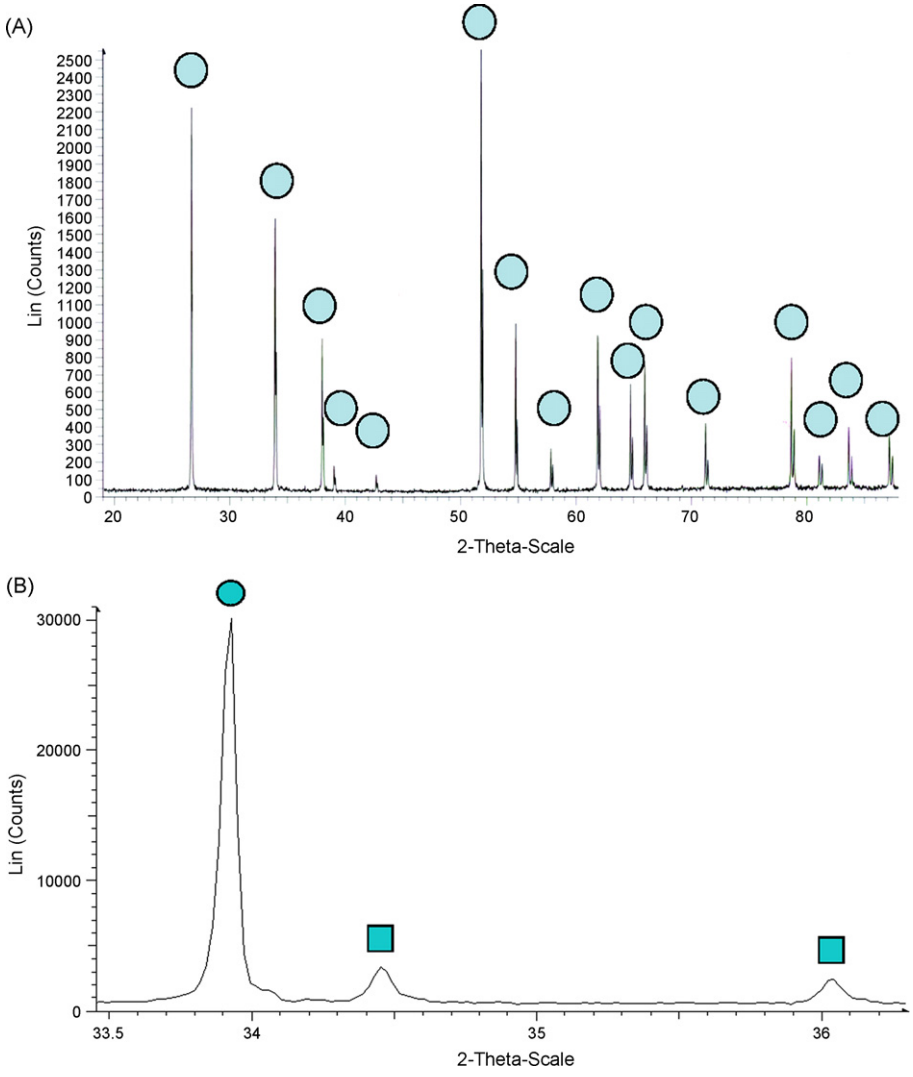

Fig. 3. Diagram of diffraction of X-rays carried out on the surface of a doped ceramics with cobalt monoxide 1%$_{wt}$ (A and B).

where A is the Richardson constant's = 1.2×10^6 A m^{-2} K^{-2}, T the temperature in Kelvin, $\beta = \sqrt{(e^3/(4\pi\varepsilon_0\varepsilon))}$ a constant related to the size of the grains and the width of the barrier of potential, e the electron charge, ε_0 and ε the permittivity of the vacuum and SnO_2, respectively, and Φ indicates the height of the barrier of potential which is stable when the current is weak and decreases brutally and in an important way when the voltage becomes higher than of threshold voltage. The calculation of the slope of the right-hand sides ($\ln J = (a/T) + B$, a and B constants) makes it possible to calculate the barrier of potential according to the following formula (Table 4; Fig. 5):

$a = \Phi/k$ with Φ the barrier of potential, k the Boltzman constant's = 1.38×10^{-23} J K^{-1} = 8.6×10^{-5} eV K^{-1}.

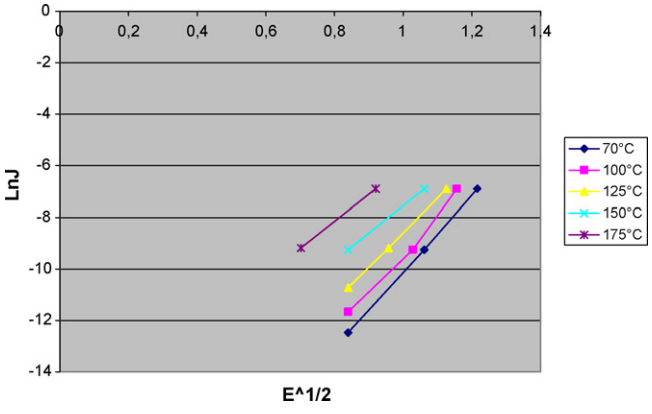

Fig. 4. Characteristic curves, $\ln J$ vs. E, of the system 99.5%$_{wt}$ SnO_2 + 0.5%$_{wt}$ CoO measured at different temperatures.

Table 4
Evolution of the potential barrier Φ in function of the cobalt amount

CoO (%)	Φ (eV)
0	–
0.05	–
0.25	0.5 ± 2
0.5	1.1 ± 2
1	0.7 ± 2
1.5	0.9 ± 2
2	0.5 ± 2

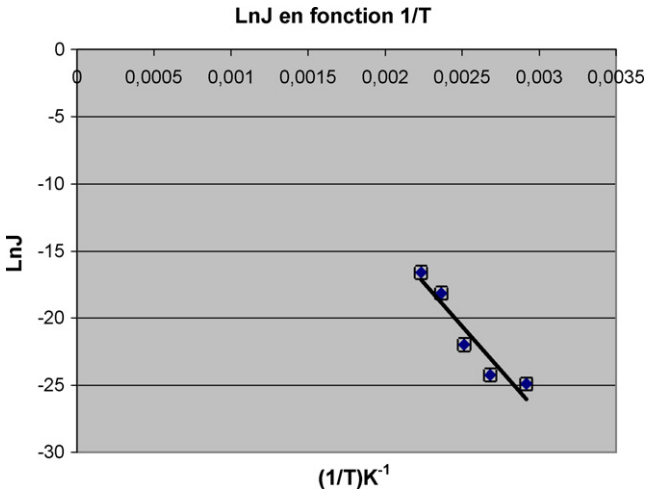

Fig. 5. Temperature influence on the current density for constant electrical field.

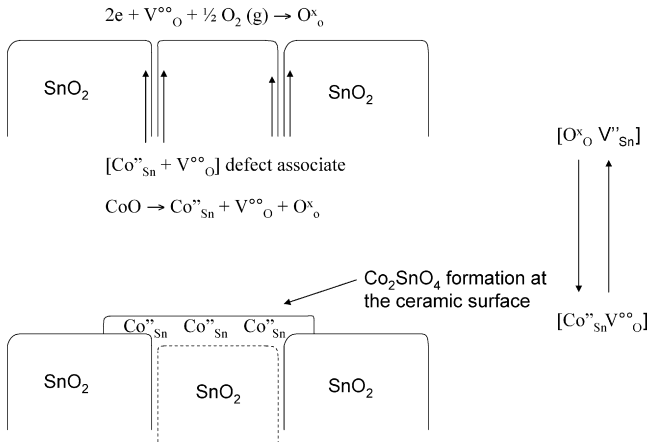

Fig. 7. Scheme of the Co_2SnO_4 formation at the ceramic surface.

The values obtained in Table 4 are of the same order of magnitude that those described within the framework of the calculation of the barrier of the varistors containing ZnO. Indeed the barrier of potential Φ is about 0.7 eV for the majority of the commercial varistors containing ZnO.[13]

Fig. 6 shows SEM images of samples. Pores and single-phase grains are observed. In backscattered image mode a precipitate appears in dark witch can be related to the presence of relatively light element concentration ($M_{Co} = 58.93$, $M_{Sn} = 118.71$, $M_O = 16$). The presence of cobalt on the surface of the ceramics shows that there was apparently mass transport towards surface during sintering. In order to investigate this light phase we carried out an X-rays diffraction analysis of the specimen surface. One of these diagrams is reported on Fig. 3B. X-ray diffraction pattern were recorded between 30° and 40° (2θ) with a scan step 0.022° and a counting time of 535 s/step. With these conditions, the phase Co_2SnO_4 is identified at the ceramic surface (Fig. 3B). Oxygen vacancies associated with Co''_{Sn} diffuses out from the interior to the surface of the sample, where the concentration of oxygen vacancies is low. Since the oxygen vacancies drag additional Co ions from the interior to the surface, the concentration of Co ions at the surface is much higher than in the bulk and exceeds the solubility limit of Co ions in SnO_2. The diffusion of a defect associate $[Co''_{Sn} + V_0^{\circ\circ}]$ allows to explain the formation of Co_2SnO_4 at the surface (Fig. 7). Nevertheless the mechanism of diffusion of such defect associate is unclear. This suggests that the diffusion is realized on the oxygen and tin sublattices without vacancies.

The realization of the electric tests on the one hand and the knowledge of the microstructure on the other hand enable us to calculate the barrier of potential by grain. Indeed, if we admit that ceramics are homogeneous with the grains of the same size (G) and that the threshold voltage of each grain boundary is constant (V_s), the sum of threshold thickness of the ceramics must be equal to the macroscopic threshold (U_s):

$$U_s = nV_s$$

with n indicates the number of grain boundaries on the thickness of the ceramic, $n = n' - 1$ (n' being the number of the grains). The average size of the grains is measured by of Mendelson's method[14] which recommends considering the average size of the grains by the formula: $G = 1.56 \times L$, with L: the average length between grain.

Table 5 shows that the voltage by grain boundary increases abruptly with cobalt monoxide. Its value is particularly high since about 10 V (generally this value is in the range: 1–4 V/barrier).[5] The addition of cobalt oxide makes it possible to lower the tension.

Fig. 2 reports the effectiveness of donor doping by depicting the dynamic apparent resistivity of the ceramic system. Isoresis-

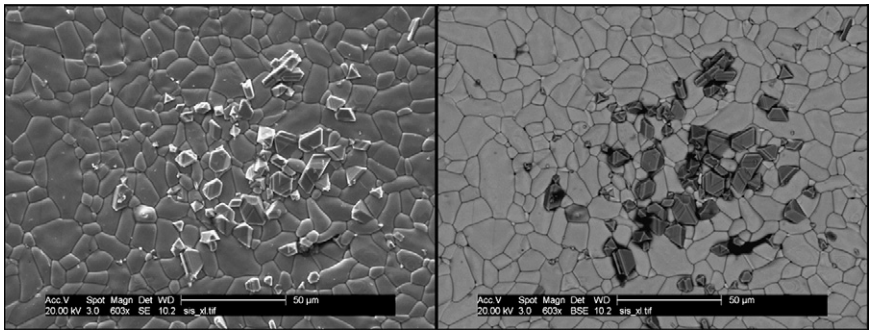

Fig. 6. SEM (secondary and backscattered images) of polycrystalline SnO_2 ceramic with $1\%_{wt}$ CoO–1623 K (2 h) (EDS analysis gives a ratio Co/Sn ≈ 0.5 for the dark grains observed on the backscattered image).

Table 5
Evolution of the grains sizes and the threshold voltages corresponding

CoO (%)	Diameter (μm)	Average grains number (experimental)	L (μm)	G (μm)	U_s (V)	Epaisseur (μm)	Theoretical grains number in the ceramic thickness	Theoretical grains boundaries number in the ceramic thickness	V_s (V)
0	243	130	2	3	90	1.20E+03	412	411	0.22
0.05	241	48	5	8	1867	1.40E+03	175	174	11
0.25	241	25	10	15	950	1.40E+03	93	92	10
0.5	241	34	7	11	817	1.50E+03	136	135	6
1	241	40	6	9	840	1.50E+03	159	158	5
1.5	241	56	4	7	880	1.50E+03	223	222	4
2	241	60	4	6	1000	1.50E+03	239	238	4

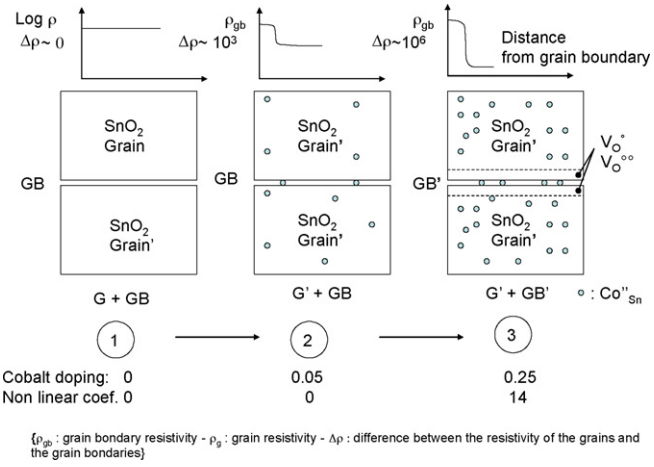

Fig. 8. Scheme of the barriers formation at the grain boundaries vs. CoO doping.

tivity lines are superimposed on the E–J curve. On doping with CoO the resistivity increases drastically from 10^4 to 10^{10} Ω cm. It appears that there is a threshold for which barriers voltage height and width trigger the nonlinear effect. A microstructure of SnO_2 grains and grain boundaries with a resistivity differential of 10^6 Ω cm appears therefore compulsory. This corresponds to $x = 0.25\%_{wt}$, such a value being the cobalt solubility in polycrystalline SnO_2. In other word, the diffusion of too small amount of cobalt in the grain of the ceramic (<0.25%$_{wt}$) does not create any nonlinear effect: the depletion layer of electrons on both sides of the grain boundary is not formed (Fig. 8).

From 0 to 0.25%$_{wt}$ CoO, the system [grain + grain boundaries] gains its nonlinearity suggesting that the conductivity differential between the grain and the grain boundaries is increased by increasing essentially the grain conductivity, the grain boundary resistivity being relatively the same.

At high current where the current is controlled by the impedance of the grain saturated by cobalt. The resistivity reaches 10^3 Ω cm. With extra CoO doping, the solubility of the grains being achieved, it is not surprising that the high current values are more or less independent of the cobalt concentration.

4. Conclusion

We studied the influence of doping by ceramics cobalt oxide containing tin dioxide. Contents ranging between 0.25% and 2% of mass were investigated. The cobalt monoxide proves to be an effective additive of sintering. However its role is optimum for 0.25%, i.e. for relatively weak doping. Additional additions are useless. The size of the grains evolves in a similar way with a maximum of 15 μm. It results from this a threshold (E_s) which increases with the cobalt content in accordance with the relation: $E_s = (e - G)/e^2 v_s$ where e is the thickness of ceramics, G the average size of the grains and v_s is the average threshold of voltage a grain boundary. In a way enough surprising, the coefficient of nonlinearity is relatively constant with the cobalt monoxide concentration whereas the calculation height of the barrier of potential and the average tension of threshold of the grain boundaries is optimum for 0.25%. Also these last two parameters do not seem to be related to the coefficient of nonlinearity. The electric characterization correlated with a study of the microstructure shows that doping with cobalt oxide is probably carried out by diffusion in the grain of ceramics in the form $Sn_{1-x}Co_xO_2$ ($CoO \rightarrow Co''_{Sn} + V_0^{\circ\circ} + (1/2)O_2(g)$) and that excess is rejected on the surface of ceramics by the grain boundaries in the mixed oxide shape Co_2SnO_4. The electric properties of ceramics are thus limited by the cobalt solubility. The conductivity of SnO_2 grains controls the difference in resistivity between the grain and the grain boundaries.

Acknowledgement

The authors are grateful for the Centre de Diffractométrie Henri Longchambon (Université Lyon1) for the powder data acquisition. This research is supported within the French Agence Nationale pour la Recherche (ANR).

References

1. Pianaro, S. A., Bueno, P. R., Longo, E. and Varela, J. A., A new SnO_2-based varistor system. *Journal of Materials Science Letters*, 1995, **14**, 692–694.
2. Li, C. P., Wang, J. F., Su, W. B., Chen, H. C., Zhong, W. L. and Zhang, P. L., Effect of Mn^{2+} on the electrical nonlinearity of (Ni, Nb)-doped SnO_2 varistors. *Ceramics International*, 2001, **27**, 655–659.
3. Kimura, T., Inada, S. and Yamaguchi, T., Microstructure development in SnO_2 with and without additives. *Journal of Materials Science*, 1989, **24**, 220–226.
4. Varela, J. A., Whittemore, O. J. and Longo, E., Pore size evolution during sintering of ceramic oxides. *Ceramics International*, 1990, **16**, 177–189.
5. Varela, J. A., Gouvéa, D., Longo, E., Dolet, N., Onillon, M. and Bonnet, J. P., The effect of additives on the sintering of tin oxide. *Solid State Phenomena*, 1992, **25–26**, 259–268.

6. Varela, J. A., Cerri, J. A., Leite, E. R., Longo, E., Shamsuzzoha, M. and Bradt, R. C., Microstructural evolution during sintering of CoO doped SnO_2 ceramics. *Ceramics International*, 1999, **25**, 253–256.
7. Dibb, A., Cilense, M., Bueno, P., Maniete, Y., Varela, J. and Longo, E., Evaluation of rare earth oxides doping SnO_2 ($Co_{1/4}$ $Mn_{3/4}$) O-based varistor system. *Materials Research*, 2006, **9**(3), 339–343.
8. Bacelar, W. K., Oliveira, M. M., Souza, V. C., Longo, E., Leite, E. R. and Varela, J. A., Influence of the oxygen adsorbed on tin varistors doped with Co, Mn and Cr oxides. *Journal of Materials Science: Materials in Electronics*, 2002, **13**, 409–414.
9. Fayat, J. and Castro, M. S., Defect profile and microstructural development in SnO_2-based varistors. *Journal of the European Ceramic Society*, 2003, **23**, 1585–1591.
10. Mizusaki, J., Koinuma, H., Shimoyama, J.-I., Kawasaki, M. and Fueki, K., High temperature gravimetric study on nonstoichiometry and oxygen adsorption of SnO_2. *Journal of Solid State Chemistry*, 1990, **88**, 443–450.
11. Kim, B.-C., Jung, J.-I., Lee, J.-H. and Kim, J.-J., Precipitate concentration of Co_2SnO_4 in CoO-doped SnO_2 ceramics at different oxygen chemical potentials. *Solid State Ionics*, 2001, **144**, 321–327.
12. Kilic, C. and Zunger, A., Origins of coexistence of conductivity and transparency in SnO_2. *Physical Review Letters*, 2002, **88**(9) (095501-1/4).
13. Cerri, J. A., Leite, E. R., Gouvéa, D., Longo, E. and Varela, J. A., Effect of cobalt (II) oxide and manganese (IV) oxide on sintering of tin (IV) oxide. *Journal of the American Ceramic Society*, 1996, **74**, 799–804.
14. Mendelson, M. I., Average grain size in polycrystalline ceramics. *Journal of the American Ceramic Society*, 1969, **52**(8), 443–446.